The following publication Z. Zhao et al., "Enabling Simultaneous DAS and DTS Through Space-Division Multiplexing Based on Multicore Fiber," in Journal of Lightwave Technology, vol. 36, no. 24, pp. 5707-5713, 15 Dec. 2018 is available at https://doi.org/10.1109/JLT.2018.2878559.

Enabling simultaneous DAS and DTS through space-division multiplexing based on multicore fiber

Zhiyong Zhao, Yunli Dang, Ming Tang, *Senior Member, IEEE,* Liang Wang, *Member, IEEE,* Lin Gan, Songnian Fu, Chen Yang, Weijun Tong, and Chao Lu, *Fellow, OSA*

***Abstract*—We have proposed and demonstrated a hybrid optical fiber sensor that enables simultaneous distributed acoustic sensing (DAS) and distributed temperature sensing (DTS). The hybrid fiber sensor is realized through space-division multiplexed (SDM) reflectometers in a multicore fiber (MCF), where Raman optical time-domain reflectometry (ROTDR) for DTS is implemented simultaneously with phase-sensitive optical time-domain reflectometry (Φ-OTDR) for DAS through space-division multiplexing. The SDM reflectometers share an identical pulse source, but use separate interrogation fiber cores, allowing simultaneous measurement of ROTDR and Φ-OTDR. The proposed hybrid sensor based on MCF does not suffer from the incompatible pump power levels issue existing in its counterpart based on single mode fiber thanks to the SDM implementation. Thus it effectively eliminates the restriction imposed by fiber nonlinear effects (e.g. modulation instability). Wavelet transform denoising method is employed to reduce the noise of temporal ROTDR traces; as a result, the worst temperature uncertainty is reduced from 4.1 °C to 0.5 °C over 5.76 km sensing range. The proposed SDM hybrid fiber sensor can realize simultaneous distributed intrusion detection and temperature monitoring. It offers great potential in long-term real-time pipeline monitoring for oil and gas industry.**

***Index Terms*—Multicore fiber, space-division multiplexing, distributed temperature sensing, distributed acoustic sensing.**

I. INTRODUCTION

Simultaneous distributed intrusion detection and temperature monitoring of pipelines are of great demand in oil and gas industry, in order to achieve real-time alarm on excavation, theft, leakage and other potential threats. Distributed optical fiber sensing has been proven to be the most promising solution in this kind of applications [1, 2]. Among them, Raman optical time-domain reflectometry (ROTDR) based distributed temperature sensing (DTS) is one of the most widely used technologies for temperature monitoring, with tens of kilometers sensing range and meter-scale spatial resolution [3]. ROTDR is only sensitive to temperature, which gives no temperature/strain cross-sensitivity and thus sufficiently ensures its reliability in the determination of temperature variation. On the other hand, Rayleigh scattering based distributed acoustic sensing (DAS) turns out to be the most promising solution for real-time intrusion detection of long-range pipelines. Based on the measurement of Rayleigh backscattering signal, phase-sensitive optical time-domain reflectometry (Φ-OTDR) has been widely investigated for vibration sensing [4]. In the monitoring of pipelines, simultaneous DTS and DAS are definitely desirable since it ensures continuous detection of intrusion events and temperature variation along the pipelines. However, it is difficult to implement the measurement of ROTDR and Φ-OTDR in a single mode fiber (SMF) at the same time, since simultaneous interrogation of spontaneous Raman scattering (SpRS) signal and Rayleigh scattering signal in the standard single mode sensing fiber is limited by the existence of nonlinear effects (e.g. modulation instability, stimulated Brillouin scattering, etc.) induced by the high pump power injected into the fiber [5, 6]. As SpRS is very weak in optical fibers and the Raman anti-Stokes signal is usually ~30 dB lower than the Rayleigh scattering signal [7, 8], the incident pump power is generally very high (several Watts) in ROTDR sensors in order to increase the SpRS intensity. However, Φ-OTDR cannot employ such high pump power since the threshold of nonlinear effects is normally lower than the required power level for ROTDR [5, 7], which restricts the maximum usable input power. The nonlinear tolerance of ROTDR is much higher than that of Φ-OTDR since ROTDR relies on the detection of power ratio of Stokes and anti-Stokes Raman backscattering and it is not sensitive to other nonlinear effects such as modulation instability while performance of Φ-OTDR can be significantly affected by waveform distortion caused by nonlinear effects. Therefore, the required pump

---

This work was supported in part by the GRF project PolyU 152168/17E of research grant council, Hong Kong SAR and 1-ZVGB, 1-YW3G, 4_BCBH of the Hong Kong Polytechnic University; National Natural Science Foundation of China under Grants 61331010 and 61722108. (*corresponding author: Ming Tang and Liang Wang*)

Z. Zhao, and C. Lu are with the Photonics Research Centre, Department of Electronic and Information Engineering, The Hong Kong Polytechnic University, Hong Kong (e-mail: zhiyong.zhao@polyu.edu.hk; chao.lu@polyu.edu.hk).

Y. Dang, M. Tang, L. Gan and S. Fu are with the National Engineering Laboratory of Next Generation Internet Access Networks, School of Optical and Electronic Information, Huazhong University of Science and Technology, Wuhan 430074, China (e-mail: m201572180@hust.edu.cn; tangming@mail.hust.edu.cn; lingan@hust.edu.cn; songnian@mail.hust.edu.cn).

L. Wang is with the Department of Electrical Engineering, The Chinese University of Hong Kong, Hong Kong (e-mail: lwang@ee.cuhk.edu.hk).

C. Yang and W. Tong are with Yangtze Optical Fiber and Cable Joint Stock Limited Company (YOFC), Wuhan 430073, China (e-mail: yangchen@yofc.com; tongweijun@yofc.com).

power levels for ROTDR and Φ-OTDR are incompatible. This has made simultaneous implementation of DTS and DAS in a single mode fiber very difficult. In order to mitigate the limitation of nonlinear effects and achieve simultaneous measurement of ROTDR and Φ-OTDR in the SMF based hybrid system, pulse coding technique has been employed to increase the signal-to-noise ratio (SNR) of the system with very special design on the used laser source in order to maintain low pump power [9]. However, it is very difficult to realize such an inter-pulse incoherence and intra-pulse coherence laser source required in that system.

Recently, multicore fiber (MCF) has been used for distributed fiber sensing, bringing unique benefits that SMFs cannot offer [10, 11], e.g. distributed curvature and 3-D shape sensing is achieved by employing the bending dependence of Brillouin frequency shift in off-center cores of the MCF [10]; temperature and strain discriminative sensing has been achieved by using the different temperature/strain responses of a heterogeneous MCF [11]. In this paper, we propose and experimentally demonstrate a MCF based space-division multiplexed hybrid fiber sensor, enabling simultaneous interrogation of DAS and DTS. In the hybrid sensing system, temperature monitoring is realized by ROTDR, and Φ-OTDR has been used for vibration detection, respectively. Thanks to multiple spatial cores embedded in the single MCF, the measurement of SpRS signal and Rayleigh scattering signal can be carried out separately in distinct cores, which successfully addresses the problem of incompatible input pump power levels in the hybrid system using SMF. In this way, simultaneous measurement of Raman and Rayleigh scattering signals is achieved by sharing the same optical components of pulse generation. Wavelet transform denoising (WTD) method has been employed to denoise ROTDR traces, which reduces the worst temperature uncertainty to 0.5 ^{o}C over 5.76 km sensing range. With the ability of simultaneous distributed intrusion detection and temperature monitoring, the proposed hybrid sensor shows great potential for long-range real-time pipelines monitoring in oil and gas industry.

II. MEASUREMENT PRINCIPLE, SETUP AND RESULTS

A. Measurement principle

Due to the constraint of incompatible input pump levels, it is difficult to implement the measurement of Φ-OTDR and ROTDR simultaneously by using SMFs. But by using a MCF, the two can be carried out separately in different cores by sharing the same pulse source with only one set of pulse generation devices, which enables simultaneous measurement of Raman and Rayleigh scattering signals. So compared with the hybrid system that uses SMF, the proposed SDM scheme will no longer suffer from the problem of incompatible input pump power levels. In the hybrid system, Φ-OTDR is used to achieve vibration detection and ROTDR is utilized for temperature monitoring. In this way, simultaneous measurements of DAS and DTS are obtained.

In a narrow linewidth coherent laser based Φ-OTDR, the Rayleigh backscattered light from a pump pulse with duration of W in the optical fiber will interfere coherently at the receiver, creating speckle-like OTDR trace with intensity governed by [12, 13]

$$\begin{aligned} P(t)=&\sum_{m=1}^{N} a_m^2 \exp\left(-2\alpha\frac{c\tau_m}{n_f}\right) rect\left(\frac{t-\tau_m}{W}\right)+ \\ &2\sum_{m=1}^{N}\sum_{n=m+1}^{N} a_m a_n \cos\phi_{mn} \exp\left\{-\alpha\frac{c(\tau_m+\tau_n)}{n_f}\right\} rect\left(\frac{t-\tau_m}{W}\right) rect\left(\frac{t-\tau_n}{W}\right) \end{aligned} \tag{1}$$

where N is the total number of scattering points; a_m and a_n are the amplitudes of the scattered waves; α and n_f are the attenuation coefficient and refractive index of fiber respectively; c is the velocity of light in vacuum; τ_m represents the round trip time from the input to the i -th scattering at z_m with $\tau_m = 2n_f z_m / c$; $\phi_{m,n}$ denotes the phase difference between the m -th, and the n -th scattering with $\phi_{m,n} = 4\pi n_f \nu (z_m - z_n)/c$, in which ν is the laser frequency. Vibration applied to the sensing fiber leads to the modification of local refractive index, which alters the phase difference $\phi_{m,n}$. As a result, the measured Rayleigh backscattered optical intensity at the perturbation point will be varied accordingly. Therefore, by measuring the intensity variation of Φ-OTDR trace, intrusion event can be monitored. Specifically, this is done by subtracting a Φ-OTDR trace with an undisturbed reference trace and hence phase change induced intensity variation can be retrieved.

On the other hand, due to the temperature dependent feature of Raman anti-Stokes signal, the temperature profile can be derived from the power ratio of Raman anti-Stokes ($I_{as}(z)$) to Stokes ($I_s(z)$) light, according to

$$\frac{I_{as}(z)}{I_s(z)} \propto \left(\frac{\lambda_s}{\lambda_{as}}\right)^4 \exp\left(-\frac{h\Delta\nu}{k_B T(z)}\right) \tag{2}$$

where λ_s , λ_{as} are the wavelength of Raman Stokes and anti-Stokes light, respectively; h is the Plank constant; $\Delta\nu$ is the frequency separation between the pump and Raman signals; k_B is the Boltzmann constant, and $T(z)$ is the fiber temperature.

B. Experimental setup

For proof of concept, a MCF containing seven cores has been used in our experiment, as shown in Fig. 1(a). While it should be pointed out that a dual-core fiber will be enough for the proposed hybrid sensing system. The MCF has 8.6±0.5 um core diameter, 150 µm cladding diameter and 42 µm core-core pitch with the outer six cores arranged hexagonally. The cores are all designed to be surrounded by deep trench and eventually the crosstalk between adjacent cores is suppressed to be as low as −45dB/100km. The measured attenuation coefficients @ 1550 nm for each core of the MCF are listed in table I.

TABLE I
THE MEASURED ATTENUATION COEFFICIENTS @ 1550 NM OF EACH CORE

Core 1	Core 2	Core 3	Core 4	Core 5	Core 6	Core 7
0.261	0.261	0.244	0.244	0.263	0.292	0.280

The unit of attenuation coefficient is dB/km.

Fig. 1(b) shows the experimental setup for the SDM Φ-OTDR and ROTDR hybrid sensor based on MCF. The narrow linewidth coherent laser diode working at 1550.1 nm has less than 1 kHz nominal linewidth. The CW output light from the laser is modulated by a semiconductor optical amplifier (SOA), which is driven by an electrical pulse generator with 30 ns rectangular pulse and 12.5 kHz repetition rate. The pulse is then amplified by an erbium-doped fiber amplifier (EDFA), and followed by an optical band-pass filter to filter out the amplified spontaneous emission (ASE) noise. The boosted pulse is then divided into two paths. The upper one is used as the pump pulse for Φ-OTDR, which is then injected into one of the outer cores. Specifically, a tunable attenuator has been inserted before the fan-in coupler in order to manage the input power, and in our experiment 24.5 dBm peak pump power for Φ-OTDR is used. The Rayleigh backscattered light is then detected by a 125 MHz photodetector. The other path is used for ROTDR with a pump pulse of 30.8 dBm power launched into the central core through the fan-in coupler. At its receiver side, the Raman Stokes and anti-Stokes components are separated by a Raman filter and eventually detected by two 125 MHz avalanche photodiode (APD), respectively. All the detectors are connected to an oscilloscope for data acquisition. The sampling rate for Φ-OTDR and ROTDR are both 100 MS/s. While it must be pointed out that the detections and acquisitions of Φ-OTDR and ROTDR are implemented separately and completely independently, so they won't affect each other at all in the hybrid system. In addition, it should be mentioned that the home-made MCF fan-in coupler has less than 1 dB insertion loss for each core. The 5.76 km MCF is divided into several segments for the convenience of applying disturbance and temperature to different locations. Both fiber segment A and B are wound into several loops with ~12 cm diameter, respectively, as shown in Fig. 1(b).

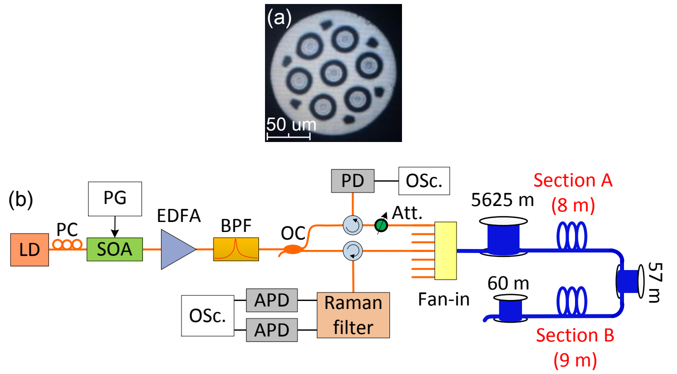

Fig. 1. (a) Cross section of the seven-core MCF; (b) experimental setup for the SDM Φ-OTDR and ROTDR hybrid sensor. LD: Laser diode; PC: polarization controller; SOA: semiconductor optical amplifier; PG: pulse generator; EDFA: erbium-doped fiber amplifier; BPF: band-pass filter; OC: optical coupler; Att.: tunable attenuator; APD: avalanche photodiode; PD: photodetector; OSc.: oscilloscope.

C. Experimental results

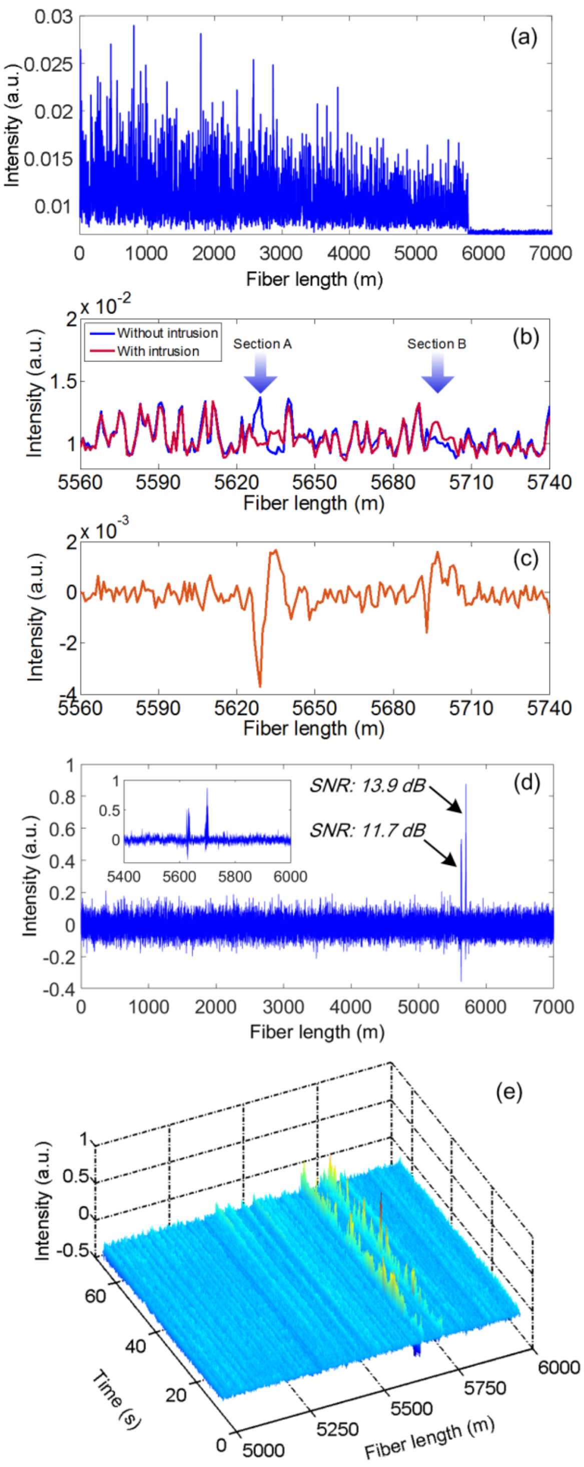

Fig. 2. (a) Typical Φ-OTDR trace along the MCF; (b) the measured traces without and with intrusion applied to fiber segment A and B, respectively; (c) the differential intensity trace obtained from (b) around segment A and B; (d) superimposed 885 consecutive differential Φ-OTDR traces when disturbances are applied at fiber segment A and B; (e) evolution of the differential Φ-OTDR trace around segment A and B as a function of time and fiber length.

Fig. 2(a) shows the typical Φ-OTDR trace acquired in our experiment. In order to get high SNR, 512 averages have been performed, which takes roughly less than one second. The intensity fluctuation results from coherent Rayleigh interference of the backscattered light within the pulse duration. The intensity distribution contains the local refractive index information of the fiber. As analyzed previously, any perturbation applied to the fiber leads to the change of local refractive index, and eventually modifies the backscattered optical intensity. Figure 2(b) shows the measured traces without and with intrusion applied to fiber segment A and B, and their differential intensity trace has been presented in Figure 2(c), where the intrusion event has been successfully retrieved from the differential intensity profile in this tentative experiment.

In order to evaluate the performance of Φ-OTDR in the proposed SDM hybrid sensing system, intrusion events were emulated by manually tapping on fiber segment A and B. Meanwhile, the Φ-OTDR traces were consecutively recorded with 100 MS/s electrical sampling rate. Note that the used 30 ns pulse duration provides 3 m spatial resolution for Φ-OTDR. Then the collected raw traces were used to subtract the reference trace to obtain differential intensity traces. Fig. 2(d) shows the superimposed 885 consecutive differential Φ-OTDR traces when disturbances are applied at fiber segment A and B. The inset shows the zoom-in view of differential traces around the disturbance locations, where intrusion events at fiber section A and B can be clearly identified. The SNR of the two peaks in the differential traces is calculated to be 11.7 dB and 13.9 dB respectively, where the SNR here is defined to be the ratio of the differential signal peak intensity (I_{peak}) over the standard deviation of noise floor (I_{noise}), i.e. SNR = 10log (I_{peak}/I_{noise}). The result also indicates that no optical intensity change occurs at undisturbed locations, verifying the excellent performance of multi-event detection and positioning of Φ-OTDR in the SDM hybrid sensing system. For better observation, the evolution of differential Φ-OTDR trace as a function of time and fiber length has been presented in Fig. 2(e). Theoretically, the maximum detectable vibration frequency is 6.25 kHz according the sampling theorem considering the used pulse repetition rate. However, due to large averaging times have been used, the actual maximum detectable frequency should be much lower, so less averaging times should be employed if one wants to retrieve the vibration frequency from the measurement of Φ-OTDR.

On the other hand, the measurement of ROTDR is implemented in parallel in the central core of MCF. Due to the weak SpRS intensity, the ROTDR traces were averaged by 52100 times, which takes about 80 seconds. However, it is found that the traces are still quite noisy which is because the used pump power is actually relatively low. In order to increase the measurement accuracy, wavelet transform denoising (WTD) technique is employed. WTD decomposes the raw signal into a series of frequency bands, then the soft thresholding is set to remove the high frequency noise components, and finally the denoised signal can be retrieved through inverse wavelet transform [14, 15]. Specifically, Daubechies 5 (db5) is used as the wavelet basis (mother wavelet) to decompose the acquired raw data for denoising in the experiment. The denoising processing takes less than one second in Matlab. Fig. 3(a) shows the measured ROTDR raw anti-Stokes power trace together with the trace after denoising by WTD. The magnified view of the trace at the middle section of MCF indicates that the trace becomes much smother after denoising, and this will lead to huge SNR enhancement. In order to verify this, the SNRs of the raw trace and the denoised trace as a function of the fiber length have been calculated, as show in Fig. 3(b), where 4.8 dB SNR improvement has been obtained at the end of the sensing fiber after denoising, which will be helpful to reduce the uncertainty of temperature determination.

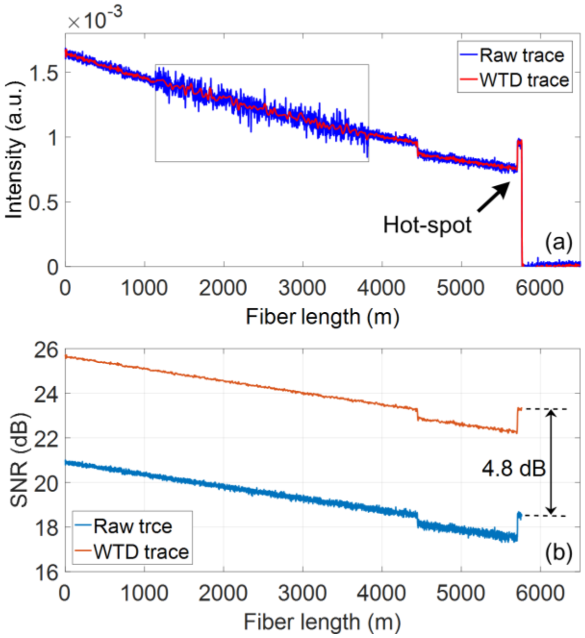

Fig. 3. (a) The measured Raman anti-Stokes traces together with the trace after denoising by WTD; (b) The SNR of the raw anti-Stokes trace and the denoised trace as a function of fiber length.

In order to evaluate the performance of ROTDR in the proposed SDM hybrid sensing system, several different temperatures (50 ^{o}C, 60 ^{o}C, 75 ^{o}C) have been applied to the last 60 m long fiber at the far end of MCF, where the fiber is immersed in an electrical water bath and different temperatures are generated by electric heating, meanwhile a mercurial thermometer is placed in the water for temperature calibration. For comparison, both the raw trace and the trace after denoising have been used to calculate the temperature profile respectively. The resolved temperature distribution around the hot-spot from the raw ROTDR traces is presented in Fig. 4(a). While that from the traces after denoising have been shown in Fig. 4(b). Note that the insets in these two figures are the complete temperature traces along the whole sensing fiber. Comparing Fig. 4(a) with Fig. 4(b), it is found that the temperature profile obtained with denoising has much less fluctuation than the one without denoising, which indicates that WTD significantly reduces the measurement uncertainty. To verify this, the temperature uncertainties along MCF without and with denoising have been compared quantitatively by calculating the temperature standard deviation with a window of 5 m fiber length, as shown in Fig. 4(c). The quadratic fitting has been applied to the traces of the calculated standard deviation, and the worst temperature uncertainties are estimated to be 4.1 °C and 0.5 °C for the cases without and with denoising, respectively. So it confirms that WTD technique can be used to enhance the SNR of the system notably and consequently improve the measurement uncertainty of ROTDR in the hybrid sensing system.

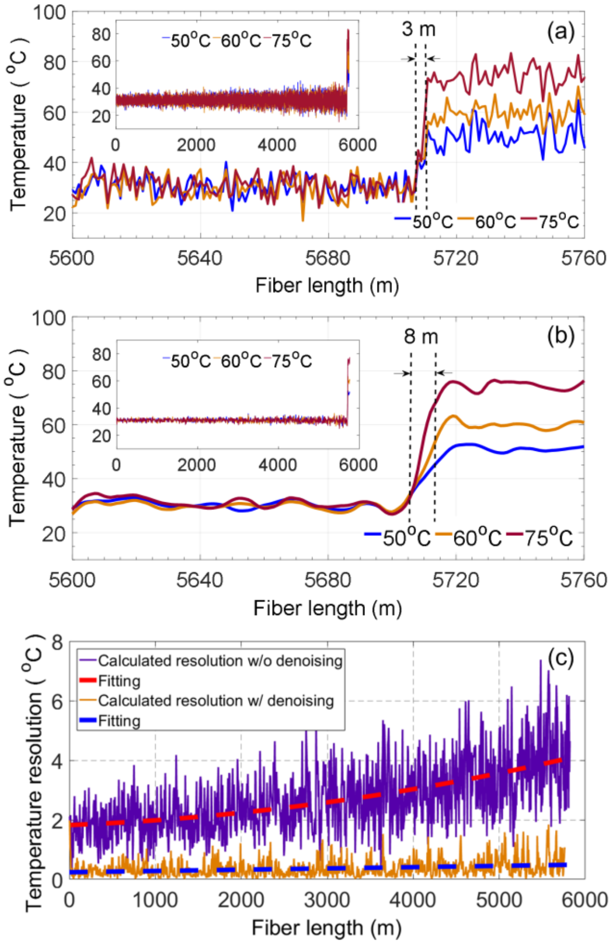

Fig. 4. (a) and (b) the resolved temperature distribution without and with denoising around the hot-spot; the insets show the temperature distribution along the whole fiber length; (c) comparison of temperature uncertainties along MCF obtained without and with denoising.

However, it must be pointed out that the improvement of SNR is achieved at the expense of degrading the spatial resolution of system that results from WTD, as have been indicated in Fig. 4(a) and 4(b), where 3 m spatial resolution is obtained for the trace without denoising, while the spatial resolution degrades to 8 m after the denoising processing. The large degradation amount of spatial resolution is mainly due to the reason that low sampling rate (100 MS/s) was used in the acquisition. But as a matter of fact, higher sampling rate will help to effectively mitigate the degradation of spatial resolution [16]. In addition, the amount of SNR improvement has also an impact on the degradation of spatial resolution, i.e. higher SNR improvement will lead to larger degradation of spatial resolution. Here the spatial resolution is defined to be the length between 10%-90% of the hot-spot rising edge.

In conventional SMF based hybrid sensing system, it is difficult to measure both the SpRS and Rayleigh scattering signals simultaneously, due to the restriction imposed by nonlinear effects. However, with the space-division multiplexed configuration using MCF, we have achieved simultaneous DAS and DTS measurement based on Φ-OTDR and ROTDR, which are implemented in different cores of the MCF.

III. DISCUSSION

In the experiment, the ROTDR is implemented in the central core of the MCF, and the Φ-OTDR is performed in one of the outer cores. However it should be pointed out that actually any core of the MCF can be used to carry out ROTDR, since the cores of MCF have the same temperature, and ROTDR is only sensitive to temperature variation but not strain nor bending. While the outer cores are preferred for the implementation of Φ-OTDR, due to the reason that vibration induced displacement leads to bending of the sensing fiber, and bending will cause tangential strain in outer cores at the bending point, which will enhance the response of system to vibration [10]. However, the central core is located in the geometric neutral axis of the fiber, bending will not generate any strain in it. So sensitivity enhanced vibration sensor can be obtained by Φ-OTDR using the outer cores in comparison with the one using the central core.

As for the sensing range of the proposed hybrid system, it is fundamentally determined by ROTDR, originating from the intrinsic weakness of SpRS. But as we have shown here, wavelet transform denoising among other image denoising techniques could significantly enhance the SNR of system and thus extending the sensing range [17]. As a matter of fact, in order to obtain longer sensing range, not only denoising post-processing but also pulse coding and distributed Raman amplification have been demonstrated [18, 19]. It is believed that the combination of all these techniques will further extend the sensing range of the hybrid system.

It should be mentioned that the hybrid sensing system can actually be achieved based only on Rayleigh scattering in MCF, where one branch could be used as DAS by performing the conventional Φ-OTDR, and the other one be used to make DTS by implementing a frequency swept Φ-OTDR and then calculate the cross-correlation of two set of measurements [20, 21]. In this case, high-sensitivity measurements of vibration and relative temperature variation will be achieved.

Finally, it should be pointed out that the use of a single MCF rather than multiple SMFs will lead to a reduction of the cost associated with embedding or attaching the sensors, a simpler and more robust sensor design and ease of installation, thanks to its integrated, compact and uniform structure along the whole fiber range. In addition, the use of MCF in this work provides a novel perspective to carry out distributed fiber sensing through SDM configuration, which offers an alternative approach to combine the advantages of various sensing techniques and opens a new way to achieve advanced sensing functionality.

IV. CONCLUSION

In conclusion, the results presented in this paper constitute the first experimental demonstration of simultaneous DAS and DTS measurement through space-division multiplexing based on MCF. With the spatially multiplexed ROTDR and Φ-OTDR hybrid sensing system in MCF, the measurement of SpRS signal and Rayleigh scattering signal has been conducted in parallel using only one set of optical pulse source, showing great improvement in comparison with the hybrid system in SMFs. In addition, ROTDR with wavelet transform denoising technique has been demonstrated with enhanced temperature monitoring performance, which reduces the worst temperature uncertainty from 4.1 °C to 0.5 °C over 5.76 km sensing range. This work provides an alternative solution of simultaneous DTS and DAS to the community, and it shows a new perspective that MCF based SDM hybrid fiber sensing system can help to provide some unique benefits that the normal SMFs based counterpart cannot offer. Due to the excellent capability of simultaneous distributed intrusion detection and temperature monitoring, the proposed SDM hybrid sensing system shows great potential for long-range real-time pipeline monitoring in oil and gas industry.

ACKNOWLEDGMENT

Z. Zhao thanks Dr. Chaodong Wang, Mr. Xuefeng Wang, Mr. Hao Wu, and Mr. Can Zhao for their helpful discussions and assistance in the experiments. The authors would like to thank the anonymous reviewers for their constructive comments and suggestions.

REFERENCES

[1] F. Tanimola and D. Hill, “Distributed fibre optic sensors for pipeline protection,” *J. Nat. Gas Sci. Eng.*, vol. 1, no. 4-5, pp. 134–143, 2009.

[2] M. Niklès, “Long-distance fiber optic sensing solutions for pipeline leakage, intrusion, and ground movement detection,” *Proc. SPIE*, vol. 7316, pp. 731602–731613, Apr. 2009.

[3] G. Bolognini, J. Park, M. A. Soto, N. Park, and F. Di Pasquale, “Analysis of distributed temperature sensing based on Raman scattering using OTDR coding and discrete Raman amplification,” *Meas. Sci. Technol.* vol. 18, no. 10, pp. 3211–3218, 2007.

[4] Y. Lu, T. Zhu, L. Chen, and X. Bao, “Distributed vibration sensor based on coherent detection of phase-OTDR,” *J. Lightw. Technol.*, vol. 28, no. 22, pp. 3243–3249, 2010.

[5] H. F. Martins, S. Martin-Lopez, P. Corredera, P. Salgado, O. Frazão, and M. González-Herráez, “Modulation instability-induced fading in phase-sensitive optical time-domain reflectometry,” *Opt. Lett*. vol. 38, no. 6, pp. 872–874, 2013.

[6] F. Peng, H. Wu, X. H. Jia, Y. J. Rao, Z. N. Wang, and Z. P. Peng, “Ultra-long high-sensitivity Φ-OTDR for high spatial resolution intrusion detection of pipelines,” *Opt. Exp.*, vol. 22, no. 11, pp. 13804–13810, 2014.

[7] Z. Zhao, Y. Dang, M. Tang, L. Duan, M. Wang, H. Wu, S. Fu, W. Tong, P. P. Shum, and D. Liu, “Spatial-division multiplexed hybrid Raman and Brillouin optical time-domain reflectometry based on multi-core fiber,” *Opt. Exp.*, vol. 24, no. 22, pp. 25111–25118, 2016.

[8] M. N. Alahbabi, Y. T. Cho, and T. P. Newson, “Simultaneous temperature and strain measurement with combined spontaneous Raman and Brillouin scattering,” *Opt. Lett*. vol. 30, no. 11, pp. 1276–1278, 2005.

[9] Y. Muanenda, C. J. Oton, S. Faralli, T. Nannipieri, A. Signorini, and F. Di Pasquale, “Hybrid distributed acoustic and temperature sensor using a commercial off-the-shelf DFB laser and direct detection,” *Opt. Lett.*, vol. 41, no. 3, pp. 587–590, 2016.

[10] Z. Zhao, M. A. Soto, M. Tang, and L. Thévenaz, “Distributed shape sensing using Brillouin scattering in multi-core fibers,” *Opt. Exp.*, vol. 24, no. 22, pp. 25211–25223, 2016.

[11] Z. Zhao, Y. Dang, M. Tang, B. Li, L. Gan, S. Fu, H. Wei, W. Tong, P. Shum, and D. Liu, “Spatial-division multiplexed Brillouin distributed sensing based on a heterogeneous multicore fiber,” *Opt. Lett.*, vol. 42, no. 1, pp. 171–174, 2017.

[12] Y. Koyamada, M. Imahama, K. Kubota, and K. Hogari, “Fiber-optic distributed strain and temperature sensing with very high measurand resolution over long range using coherent OTDR,” *J. Lightw. Technol.*, vol. 27, no. 9, pp. 1142–1146, 2009.

[13] Y. Dang, Z. Zhao, M. Tang, C. Zhao, L. Gan, S. Fu, T. Liu, W. Tong, P. P. Shum, and D. Liu, "Towards large dynamic range and ultrahigh measurement resolution in distributed fiber sensing based on multicore fiber," *Opt. Exp.*, vol. 25, no. 17, pp. 20183-20193, 2017.

[14] M. Wang, H. Wu, M. Tang, Z. Zhao, Y. Dang, C. Zhao, R. Liao, W. Chen, S. Fu, C. Yang, W. Tong, P. P. Shum, and D. Liu, “Few-mode fiber based Raman distributed temperature sensing,” *Opt. Exp.*, vol. 25, no. 5, pp. 4907–4916, 2017.

[15] H. Wu, M. Tang, M. Wang, C. Zhao, Z. Zhao, R. Wang, R. Liao, S. Fu, C. Yang, W. Tong, P. P. Shum, and D. Liu, "Few-mode optical fiber based simultaneously distributed curvature and temperature sensing," *Opt. Exp.*, vol. 25, no. 11, pp. 12722-12732, 2017.

[16] H. Wu, L. Wang, Z. Zhao, N. Guo, C. Shu, and C. Lu, "Brillouin optical time domain analyzer sensors assisted by advanced image denoising techniques," *Opt. Exp.*, vol. 26, no. 5, pp. 5126-5139, 2018.

[17] M. A. Soto, J. A. Ram´ırez, and L. Thevenaz, “Intensifying the response of distributed optical fibre sensors using 2d and 3d image restoration,” *Nature Commun.*, vol. 7, 2016.

[18] M. A. Soto, T. Nannipieri, A. Signorini, A. Lazzeri, F. Baronti, R. Roncella, G. Bolognini, and F. Di Pasquale, “Raman-based distributed temperature sensor with 1 m spatial resolution over 26 km SMF using low-repetition-rate cyclic pulse coding,” *Opt. Lett.*, vol. 36, no. 13, pp. 2557–2559, 2011.

[19] G. Bolognini, J. Park, M. A. Soto, N. Park, and F. Di Pasquale, “Analysis of distributed temperature sensing based on Raman scattering using OTDR coding and discrete Raman amplification,” *Meas. Sci. Technol.*, vol. 18, pp. 3211–3218, 2007.

[20] X. Lu, M. A. Soto, and L. Thévenaz, “MilliKelvin resolution in cryogenic temperature distributed fibre sensing based on coherent Rayleigh scattering,” Proc. SPIE, vol. 9157, p. 91573R, 2014.

[21] X. Lu, M. A. Soto, and L. Thévenaz, “Temperature-strain discrimination in distributed optical fiber sensing using phase-sensitive optical time-domain reflectometry,” *Opt. Exp.*, vol. 25, no. 14, pp. 16059–16071, 2017.